Formulation of A Full Dynamic Transport Model for Heterostructure Devices *

R. Khoie
Department of Electrical and Computer Engineering
University of Nevada, Las Vegas
Las Vegas, NV 89154

Abstract

A Full Dynamic Transport Model consisting of the Momentum Conservation, Energy Conservation, and Particle Conservation Equations, along with Poisson Equation is presented. In this model, the velocity and energy of carriers are taken as *variables* of the system. The resulting system of equations are numerically solved for electrostatic potential, carriers energies, carries velocities, and carriers densities. Most Drift-Diffusion models are based on the fundamental assumption that the transport parameters such mobility, diffusion constant, and drift velocity are constant throughout the structure under any applied biasing conditions. In heterostructures, however, specially in $Al_xGa_{1-x}As/GaAs$ heterostructures, where the velocity-field characteristics exhibit the velocity overshoot, the assumption of constant mobility becomes seriously invalid. The Full Dynamic Transport Model (FDTM) presented here is a nonlinear model incorporating carriers velocities and energies, which eliminates the necessity of calculating the carriers mobilities and diffusion constants. The hot electron phenomena, such as velocity overshoot, have been accounted for by including the third moment of Boltzmann Transport Equation, which provides for energy conservation.

The results of the simulations of a one-dimensional p-n heterojunction are presented. The simulations are performed for different emitter doping levels. It has been found that by increasing the emitter doping from $10^{16}cm^{-3}$ to $5x10^{17}cm^{-3}$, the turn-on voltage of an $Al_{0.3}Ga_{0.7}As/GaAs$ heterojunction diode increases from $1.09V$ to $1.44V$ which is consistent with the results reported by others [1] – [4]. The Maximum velocity of electrons reduces from $2.5x10^7cm/sec$ to $1.8x10^7\ cm/sec$, which is due to the increased collision of electrons with doping impurities. This is also the reason for increased electron average energy from $270mev$ to $640mev$. We also observed a significant velocity overshoot in the vicinity of the space charge region of the device. The results obtained are in good agreement with the experimental and simulated results reported by others [1] – [6].

I. The Full Dynamic Transport Model

Most Drift-Diffusion (DD) models presently available in the literature are based on a thermal equilibrium approximation.[3] – [6] The DD models are linear-velocity models in which the electrons are assumed to be subject to a drift force and a diffusive force, and the electron velocity is: $v_n = -\mu_n E - \frac{D_n}{n}\nabla n$. The main difficulty with this approach is in accurate estimation of electron mobility and diffusion constant. Also, in DD models, the effects of high field electron dynamics are neglected due to the thermal equilibrium assumption.

The Full Dynamic Transport Model (FDTM) presented here, is a nonlinear model involving the carriers velocities and average energies, which eliminates the necessity of calculating the mobility and

*This research was supported by the U.S. Army Research Office under ARO Grant No. DAAL 03-87-G-0004

diffusion constants. The particle, momentum, and energy conservations, and Poisson equations are given, respectively, by:

$$\frac{\partial n}{\partial t} + \nabla.(nv) = -R \tag{1}$$

$$\frac{\partial v_n}{\partial t} = -\frac{qE}{m_n} - \frac{2}{3m_n n}\nabla(nw_n) - v_n\nabla.v_n + \frac{1}{3n}\nabla(nv_n^2) + \frac{v_n}{\tau_m} \tag{2}$$

$$\frac{\partial w_n}{\partial t} = -q(v_n \cdot E) - v_n(\nabla w_n) - \frac{2}{3n}\nabla \cdot (nv_n(w_n - \frac{m_n}{2}v_n^2)) - \frac{\nabla}{n}Q_T - (\frac{\partial w}{\partial t})_{coll} \tag{3}$$

$$\nabla.E = \frac{q}{\epsilon}(p - n + C) \tag{4}$$

In the above equations the subscript n represents the variables associated to electrons; with v and w as carrier velocity and average energy, respectively.

In Eq. (1) the term R is the rate of recombination of electrons through traps. In Eq. (2), τ_m is the momentum relaxation time, the term $(-\frac{qE}{m_n})$, is the acceleration due to the crystal potential and the external electric field. The second term, $(-\frac{2}{3m_n n}\nabla(nw_n))$, represents the diffusive acceleration, which forces electrons to move in the direction that minimizes the concentration and energy of electrons. The third term, $(-v_n\nabla.v_n)$, causes convective electron flow, giving electrons a tendency to move to an area where electrons move the fastest. The term $(\frac{1}{3n}\nabla(nv_n^2))$ is due to the kinetic energy of electrons. The last term, $(-\frac{v_n}{\tau_m})$, accounts for collisions. The right hand side of Eq. (3) describes how individual forces contribute to changes in the total energy of electrons: the first term, $(-q(v_n \cdot E))$ corresponds to the contribution of the electric field, and the second term, $(-v_n(\nabla w_n))$ is due to the convection of energy flow. The third term, $(-\frac{2}{3n}\nabla \cdot (nv_n(w_n - \frac{m_n}{2}v_n^2)))$, is a combination of the second and fourth terms in Eq. (2). The term $-\frac{\nabla}{n}Q_T$ accounts for the gradients of heat generation, and it is assumed to be negligible. This assumption has been shown to be valid when the distribution function is symmetrical about some mean value in the momentum space, which implies that the temperature is constant throughout the device [7]. The last term, $(-(\frac{dw}{dt})_{coll})$, is the change in energy due to collisions, and is represented by $\frac{w-w_0}{\tau_w}$, where τ_w is the energy relaxation time, and w_0 is the initial average electron energy equal to $\frac{3}{2}kT_o$, and T_o is the effective electron temperature.

In this paper, we study a steady-state case only, and make the assumptions that others [7]-[8] have made, namely, neglecting the convective term, $v\nabla v$, and the terms with the kinetic energy, $\frac{1}{2}mv^2$. The reason for neglecting $\frac{1}{2}mv^2$ is that the total energy : $w = \frac{3}{2}kT_o + \frac{1}{2}mv^2$, and at room temperature the kinetic energy is negligible compared to the thermal energy. Equations similar to Eqs. (1) through (3) are written for holes, providing a system of *seven* equations and *seven* unknowns which is numerically solved for: $\psi, n, p, v_n, v_p, w_n$, and w_p. Auxiliary equations (such as rate of recombination through traps) are used in each iteration cycle.

II. Results and Conclusions

A $n - Al_{0.3}Ga_{0.7}As/p - GaAs$ heterojunction device with $10^{16}/cm^{-3}$ of n-type emitter doping, and 1 μm of emitter thickness is simulated at 300°K. The doping level and thickness of the p-type base are also $10^{16}/cm^{-3}$, and 1 μm, respectively. The simulation program begins with an initial guess for the charge density (ρ), that is used to calculate the electrostatic potential, ψ, by solving the Poisson Equation. The remaining six differential equations are then numerically solved and values of carriers concentrations, energies, and velocities are calculated. A new value for ρ is recalculated from the new n, and p, and Poisson Equation is solved again. When convergence is achieved (with the current value of variables being within 1% of the previous iteration), we proceed to calculate the current densities.

Fig.(1a) shows the electrostatic potential, ψ, in the device for different applied voltages ranging from 1.2 V to -2.2 V. As expected, the width of the space charge region decreases as the forward applied voltage increases. Also, there is no discontinuity of ψ at the heterojunction. Figs. (1b), (1c), and (1d) show the electron concentration n, electron velocity v_n, and electron energy w_n, respectively, throughout the device for different applied voltages ranging from a forward bias voltage of $1.2V$ to a reverse bias of $-2.2V$. There is a discontinuity in the electron density at the heterojunction which is due to ΔE_c. In the n-type region the electron concentration is basically equal to N_D, the donor concentration. In the p-type region the electron concentration depends on the applied voltage.

The electron velocity (Fig 1c) shows the overshoot effect at both ends of the space charge region. There is a large change in the electron velocity at the heterojunction due to different characteristics of the two materials. Also, as the width of the space charge region decreases, the peak value of the electron velocity in the center of the space charge region decreases due to the fact that electrons do not reach the saturation velocity. At the center of the space charge region, the carrier velocity saturates, but the carrier energy increases due to the increase in the electric field.(Fig. 1d) This is because the total energy of the electrons depends on the potential and the kinetic energy. The potential energy dependents on the electric filed which is the highest at the center of the space charge region.

The $i - v$ characteristic of device is shown in Figure (2a). The turn-on voltage is about 1.0 V, and the current increases somewhat exponentially as the voltage increases. To investigate the effects of doping, we increased the doping levels of both sides of the junction from $10^{16}cm^{-3}$ to $5\text{x}10^{17}cm^{-3}$. As shown in Fig. (2b) the turn-on voltage increases from 1.09 V to 1.44 V as the doping level is increased, which is consistent with the results reported by others [1] – [4]. The maximum electron velocity decreases from $2.5\text{x}10^7 cm/sec$ to $1.8\text{x}10^7 cm/sec$ at the edge of the space charge region in the GaAs. This is due to the fact that the increased scattering rate with the ionized impurities tends to slow down the electrons. As the doping level increases, the electron average energy increases from $270mev$ to $640mev$. This is due to the field dependency of the electron energy. The results obtained from our model agrees well with those published by others. (See Tomizawa [9].) Specifically, the velocity overshoot effect that occurs at about $2.0kV/cm$ agrees well with those reported by [9]. The maximum electron velocity has been reported to be $0.7\text{x}10^7 cm/sec$ in $Al_{.3}Ga_{.7}As$ and $2.2\text{x}10^7 cm/sec$ in $GaAs$.[9] From our simulations we obtained a maximum electron velocity of $0.6\text{x}10^7 cm/sec$ for $Al_{.3}Ga_{.7}As$ and $2.5\text{x}10^7 cm/sec$ for $GaAs$. This maximum velocity reduces from $2.5\text{x}10^7 cm/sec$ to $1.8\text{x}10^7$ cm/sec, with increase in doping, which is due to the increased collision of electrons with doping impurities. This is also the reason for increased electron average energy from $270mev$ to $640mev$.

References

1. G. Gao, *IEEE Trans. on Electron Dev.*, Vol. ED-38, No. 2, pp. 185-195, 1991.
2. D. B. Slater, *IEEE Electron Dev. Lett.*, Vol. 12, No. 2, pp. 54-56, 1991.
3. P. D. Rabinzohn, *IEEE Trans. on Electron Dev.*, Vol. ED-38, No. 2, pp. 222-230, 1991.
4. G. Gao, *IEEE Trans. on Electron Dev.*, Vol. ED-37, No. 5, pp. 1199-1207, 1990.
5. Y. Hiraoka, J. Yoshida, *IEEE Trans. on Electron Dev.*, Vol. ED-35, No. 7, pp. 857-862, 1988.
6. K. Yokoyama, *IEEE Trans. on Electron Dev.*, Vol. ED-31, No. 9, pp. 1222-1229, 1984.
7. N. Goldsman J. Frey, *IEEE Trans. on Electron Dev.* Vol. ED-35, No. 9, pp. 1524-1529, 1988.
8. E. M. Azoff, *Solid State Electronics* Vol. 30, No. 9, pp. 913-917, 1987.
9. K. Tomizawa, *IEEE Trans. on Electron Dev.* Vol. ED-37, No. 3, pp. 519-529, 1990.

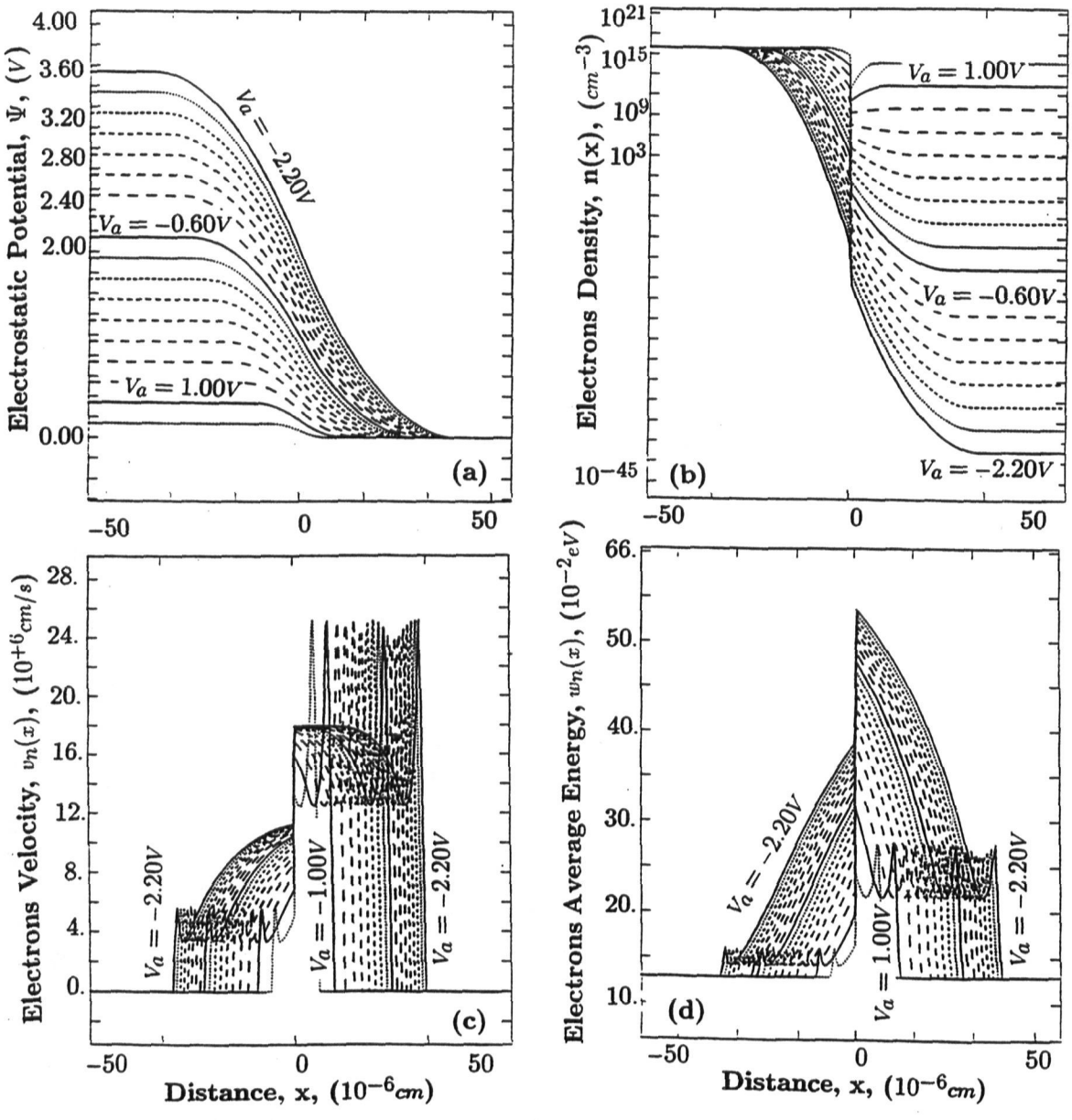

Figure 1: (a) Electrostatic potential, (b) electron density, (c) electron velocity, and (d) electron energy for different applied voltages ranging from forward +1.2 V to reverse −2.2 V, for the device with emitter doping of $10^{16}Cm^{-3}$.

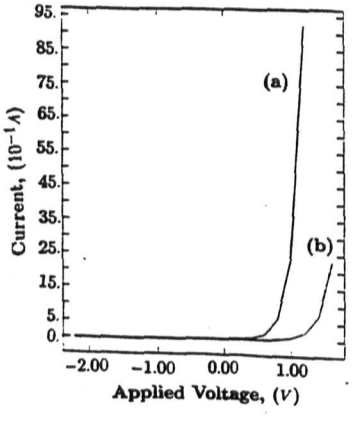

Figure 2: The $i - v$ characteristics of the device with emitter doping of (a) $10^{16}Cm^{-3}$, and (b) $5x10^{17}Cm^{-3}$.